

MIT Open Access Articles

ERK and p38 MAPK Activities Determine Sensitivity to PI3K/mTOR Inhibition via Regulation of MYC and YAP

The MIT Faculty has made this article openly available. **Please share** how this access benefits you. Your story matters.

Citation: Muranen, Taru et al. "ERK and P38 MAPK Activities Determine Sensitivity to PI3K/mTOR Inhibition via Regulation of MYC and YAP." *Cancer Research* 76, 24 (October 2016): 7168–7180 © 2016 American Association for Cancer Research (AACR)

As Published: <http://dx.doi.org/10.1158/0008-5472.CAN-16-0155>

Publisher: American Association for Cancer Research (AACR)

Persistent URL: <http://hdl.handle.net/1721.1/116784>

Version: Author's final manuscript: final author's manuscript post peer review, without publisher's formatting or copy editing

Terms of use: Creative Commons Attribution-Noncommercial-Share Alike





Published in final edited form as:

Cancer Res. 2016 December 15; 76(24): 7168–7180. doi:10.1158/0008-5472.CAN-16-0155.

ERK and p38 MAPK activities determine sensitivity to PI3K/mTOR inhibition via regulation of MYC and YAP

Taru Muranen¹, Laura M. Selfors¹, Julie Hwang¹, Lisa L. Gallegos¹, Jonathan L. Coloff¹, Carson C. Thoreen^{2,3,4,5,#}, Seong A. Kang^{2,3,4,5,\$}, David M. Sabatini^{2,3,4,5}, Gordon B. Mills⁶, and Joan S. Brugge^{1,*}

¹Department of Cell Biology and Ludwig Center at Harvard, Harvard Medical School, Boston, MA

²Whitehead Institute for Biomedical Research and Massachusetts Institute of Technology, Department of Biology, Cambridge, MA

³Howard Hughes Medical Institute, Department of Biology, Massachusetts Institute of Technology, Cambridge, MA

⁴Koch Institute for Integrative Cancer Research, Cambridge, MA

⁵Broad Institute of Harvard and Massachusetts Institute of Technology, Cambridge MA

⁶Department of Systems Biology, The University of Texas MD Anderson Cancer Center, Houston, TX

Abstract

Aberrant activation of the PI3K/mTOR-pathway is a common feature of many cancers and an attractive target for therapy, but resistance inevitably evolves as the case for any cancer cell targeted therapy. In animal tumor models, chronic inhibition of PI3K/mTOR initially inhibits tumor growth, but over time, tumor cells escape inhibition. In this study, we identified a context-dependent mechanism of escape whereby tumor cells upregulated the proto-oncogene transcriptional regulators c-MYC and YAP1. This mechanism was dependent on both constitutive ERK activity as well as inhibition of the stress kinase p38. Inhibition of p38 relieved proliferation arrest and allowed upregulation of MYC and YAP through stabilization of CREB. These data provide new insights into cellular signaling mechanisms that influence resistance to PI3K/mTOR inhibitors. Furthermore, they suggest that therapies that inactivate YAP or MYC or augment p38 activity could enhance the efficacy of PI3K/mTOR inhibitors.

Keywords

PI3K/mTOR; drug resistance; MYC; YAP; p38 MAPK; KRAS; ERK

*Corresponding author: Joan S. Brugge, Department of Cell Biology, 240 Longwood Ave. Boston, MA, Phone: 617 432-3974, Fax: 617 432-3969, joan_brugge@hms.harvard.edu.

#Current address: Department of Cellular and Molecular Physiology, Yale University School of Medicine, New Haven, CT

\$Current address: Navitor Pharmaceuticals, Cambridge, MA

Disclosure of conflicts of Interests: None

Introduction

The PI3K/mTOR (Phosphatidylinositol-4,5-bisphosphate-3-kinase/mechanistic-Target-of-Rapamycin) pathway is a major growth signaling pathway that regulates a wide variety of cellular processes, such as protein, nucleotide and lipid synthesis (1). Mutations in several oncogenes or loss of tumor suppressors lead to deregulated PI3K/mTOR-signaling in tumors (for reviews see (2, 3)), making it an attractive target for therapy. Although single agent inhibition of PI3K/mTOR typically leads to cytostasis, it has not led to durable response rates, rarely inducing tumor cell death or shrinkage of solid tumors (reviewed in (4)). Under cytostasis, tumors can relapse due to emergence of resistant cells that escape proliferative suppression through genetic or epigenetic mechanisms.

Upregulation of receptor tyrosine kinases (RTKs) (5–10) is a known resistance mechanism that allows cancer cells to survive PI3K/mTOR inhibition. Upregulation of RAS/MEK/ERK-pathway can also promote resistance to PI3K/mTOR inhibitors (6, 11, 12). Other reported mechanisms include modulation of RSK3/4 (13), c-MYC (14, 15), β -catenin (16), eIF4E (15, 17), or deregulation of 4EBP proteins (18–20). Although these alterations promote survival, the mechanism by which tumor cells overcome proliferation arrest induced by PI3K/mTOR inhibitors is not well understood. Here, we identify upregulation of c-MYC and yes-associated protein (YAP1) as a resistance mechanism that allows proliferation under chronic PI3K/mTOR inhibition. MYC and YAP upregulation is context-dependent, occurring in an activated RAS/ERK-background, and requires suppression of the stress-activated p38 MAPK (*MAPK14*).

Materials and Methods

Antibodies and Reagents

Rapamycin (gift from Dr. Blenis), BEZ235 (Axon-Medchem) and Torin1 (Tocris-Bioscience) were dissolved in DMSO and used at indicated concentrations. BEZ235 was used at 0.5 μ M except where noted differently. SB203580/SB202190 (Cell Signaling Technologies) were used at 5 μ M concentration, and cells were pre-incubated with the inhibitor 24h. UO126 (Sigma) was used at 10 μ M. MK2206, BKM120, GDC0941 (Selleck) were all used at 250nM. All antibodies are described in supplemental materials.

Plasmids/shRNAs

shRNAs were obtained from RNAi Consortium (clone IDs from Open BioSystems). pLKO *MYC* shB5 (TRCN0000039639), *MYC* shB6 (TRCN0000039640) and shB8 (TRCN0000039642), *YAP1* shF5 (TRCN0000107265) and shF8 (TRCN0000107268), *KRAS* shA8 (TRCN0000033261), shA9 (TRCN0000033262) and pLKO scrambled were used in shRNA experiments. Plasmids for over-expression of *MYC* and *YAP1* were pBABE *YAP1* (Addgene#15682), pWZL *MYC* (Addgene#10674) and *CREB1* WT in pQCXIB. pcDNA-*p38CA* (*p38/Mapk14*) was a kind gift from Dr. Aguirre-Ghiso.

RPPA Analysis

RPPA sample preparation, normalization of data points, and analysis were performed as previously described (21). Cell lysates were arrayed on slides, incubated with antibodies and quantified. Differentially expressed proteins and phospho-proteins were identified using t-test or ANOVA and $p < 0.05$ threshold. Heatmaps were generated using Cluster3.0 and Java TreeView1.1.1. Proteins were ordered by the rank-sum of the normalized values.

Cell culture

MCAS, OVCAR5, OvCa432, MDA-MB-468, MCF7 and TOV21G lines were from Dr. Slamon (UCLA) between 2008 and 2012 and validated by short tandem repeat (STR) profiling. HeLa, HCT116 and cancer lines in Figure 6 were from Dr. Sabatini (Whitehead/MIT) obtained in 2013, and 19 of the 27 lines were validated by STR at the time. HeLa, A431, DLD1, DU-145, PC3, BT549, SK-MEL-28, SW620 and S462 have not been profiled. Jeko is of unknown lineage. 3D experiments were performed as described before [8]. Detailed description is in supplemental methods. Lentiviral vectors encoding shRNAs in pLKO-plasmids were generated in 293T cells and retroviruses were generated in 293GPGs according to standard protocol (22).

Xenograft experiments

500,000 (HCT116) or million cells (OVCAR5) in 1:1 mix of PBS:Matrigel were injected subcutaneously into two flanks of ~24g 10–12 week-old female NOD.CB17-Prkdc^{scid}/J mice (Jackson labs). Once tumors became palpable (~250mm³), 12d (HCT116) or 28d (OVCAR5), mice were randomized to groups of five for each treatment group (20 animals in total). Five animals per group were calculated to give sufficient statistical power for the purpose of this experiment. Drug was administered daily intra-peritoneally. GNE493 (Genentech) (10mg/kg) was dissolved in 0.5% methylcellulose/0.2% Tween-80. Tumors were harvested on 11–13d post-treatment. All mouse studies were conducted through Institutional Animal Care and Use Committee (IACUC)-approved animal protocols (#04004) in accordance with Harvard Medical School institutional guidelines.

Immunofluorescence and microscopy

3D spheroids were fixed, stained and imaged as previously described (23). Paraffin embedded tumor sections were unmasked by pH6 citrate-buffer and probed overnight with primary antibodies. Secondary antibodies were with Alexa-488, and –568 (Invitrogen). Cells were imaged with confocal microscopy, more detailed description is in supplemental methods.

Western blot

Cells were harvested for Western in RIPA-buffer supplemented with protease and phosphatase inhibitors and MG132 (Sigma). Lysates were boiled in 1× sample buffer for 5min, resolved by 4–20% SDS-PAGE gradient gels, transferred PVDF membranes (Whatman), blocked with 5% BSA-TTBS, and probed by primary antibodies o/n. Membranes were probed with secondary antibodies linked to horseradish peroxidase.

Results

We previously showed using 3D spheroid cultures that treatment of matrix-adherent cancer cells with PI3K/mTOR inhibitors results in inhibition of cell proliferation but rarely in cell death (8). To model progression under conditions of chronic PI3K/mTOR inhibition in 3D, we cultured MCAS tumor cells under chronic exposure to the dual PI3K/mTOR inhibitor, BEZ235. Cells were cultured in reconstituted basement membrane proteins (3D), during which time the drugs and media were replenished every four days. Due to the sequestration of BEZ235 in 3D cultures, we used BEZ235 at 0.5–1 μ M concentration to fully inhibit the pathway (Supplemental Fig. 1A). MCAS cells initially displayed cytostasis in the presence of BEZ235. However, after one year of chronic exposure, proliferative outgrowths emerged (Fig. 1A lower panel), whereas control cells cultured in 3D for the same amount of time in the absence of drug remained sensitive to BEZ235 (Fig. 1A, top panel). After proliferation became apparent, the resistant cells (MCAS-R) were passaged by trypsinization every two weeks and maintained constitutively as 3D cultures in the presence of BEZ235, and the sensitive cells were maintained in DMSO (MCAS-S).

To verify that the MCAS-R outgrowths were due to proliferation, we stained for the proliferation marker Ki67 in 3D (Fig. 1B), and analyzed cell numbers in 3D at indicated timepoints (Fig. 1C and D). Although the baseline proliferation rate of vehicle-treated MCAS-R cells was lower than that of MCAS-S cells (Fig. 1C), the MCAS-R cells displayed significant proliferative advantage in the presence of BEZ235 (Fig. 1D, Tukey HSD $p < 0.01$). This effect was not limited to BEZ235, as MCAS-R cells also proliferated in the presence of a structurally distinct mTOR inhibitor, Torin1 (Fig. 1D, Tukey $p < 0.05$), and with combination of BEZ235 and Rapamycin (Fig. 1D, Tukey $p < 0.01$). To eliminate altered drug metabolism or efflux as potential mechanisms of resistance, we evaluated whether BEZ235, Torin and Rapamycin still inhibit mTOR target molecules (p-S6, p-AKT and p-4EBP1). Indeed, all inhibitors suppressed phosphorylation of these proteins (Fig. 1E). However, MCAS-R cells consistently displayed slightly higher levels of translation regulator 4EBP and phospho-4EBP1 under BEZ235-treated conditions. This is not surprising given previous reports demonstrating that minimal recovery of cap-dependent translation is needed for mTOR inhibitor resistance (15, 18–20).

The simultaneous emergence of MCAS-R cell outgrowths in several spheroids suggests that this is not a rare genetic event, but a time-dependent adaptation to chronic PI3K/mTOR inhibition. Consistent with this hypothesis, full exome-sequencing ($>830\times$ coverage/cell line) failed to identify non-synonymous or splicing variants that are discordant between MCAS-R and MCAS-S cells (24) (NCBI Sequence-Read-Archive Accession #SRP057514). Although epigenetic or non-exon alterations that might contribute to resistance cannot be ruled out, this data, together with the evidence that MCAS-R cells revert to drug-sensitive state after 16 weeks of drug-free culture (Supplemental Fig. 1B), led us to investigate alternative mechanisms of resistance. To examine a broad array of signaling pathways that could mediate resistance, we performed reverse phase protein arrays (RPPA) on lysates from MCAS-S and MCAS-R cells treated in 3D cultures with DMSO or BEZ235. We then evaluated which proteins were differentially altered under any condition (Fig. 2A). Signals from several proteins or phospho-proteins differed significantly in BEZ235-treated MCAS-R

and MCAS-S cells, however many of these also differed under basal DMSO-treated conditions (Fig. 2A, Supplemental Fig. 1C). 58 proteins were significantly differentially altered in expression or phosphorylation by BEZ235-treatment in one of the two lines (Fig. 2B, $p < 0.05$ BEZ235-treated MCAS-R vs. BEZ235-treated MCAS-S cells). Two proteins previously reported to promote resistance to PI3K/mTOR inhibitors, MYC and eIF4E, were significantly upregulated by BEZ235 treatment in MCAS-R cells relative to MCAS-S cells (Fig. 2A and B), but were not significantly changed at baseline. Similarly, several other proteins, including EGFR, paxillin, NF2, Cyclin E, caveolin1 and YAP were also differentially upregulated by BEZ235 in MCAS-R cells with minimal differences at baseline (Fig. 2B). The RPPA results for several upregulated proteins were validated by Western blot (Fig. 2C and Supplemental Fig. 1D).

Since MYC and YAP, the Hippo-pathway effector (for reviews (25, 26)), are well-recognized regulators of cell proliferation, we focused on these two proteins and examined whether their modulation would be sufficient to impact the sensitivity to BEZ235. We first evaluated whether other structurally distinct PI3K/mTOR (GNE493) or mTOR (Torin1) inhibitors induce similar changes as observed with BEZ235 in 3D and observed upregulation in both YAP and MYC (Supplemental Fig. 1E). We next addressed whether overexpression of YAP and/or MYC in the parental MCAS cells would be sufficient to overcome proliferative suppression induced by BEZ235 under standard monolayer culture conditions (2D). Although overexpression of either YAP or MYC alone promoted growth in the presence of BEZ235 (Fig. 2D and Supplemental Fig. 2A, $p < 0.01$), concurrent overexpression of MYC and YAP significantly enhanced proliferation of MCAS cells compared to overexpression of either one alone (Fig. 2D, $p < 0.01$).

We also examined whether the ability of MCAS-R cells to evade proliferative suppression induced by BEZ235 was dependent on YAP or MYC. Although shRNA knockdown of YAP or MYC resulted in significant proliferation inhibition of BEZ235-treated MCAS-R cells in 3D (Supplemental Fig. 2B and C), knockdown of either one of these genes also impaired proliferation in the DMSO control cells, indicating that MYC and YAP are required for proliferation under 3D culture conditions. Thus, we were unable to assess the effects of YAP or MYC knockdown on BEZ235 resistance in MCAS-R cells in 3D. Interestingly, knockdown of YAP did not significantly impair proliferation of DMSO-treated parental MCAS cells grown as 2D cultures (Supplemental Fig. 2D). Since MYC has previously been reported to promote resistance to PI3K/mTOR inhibitors (14, 15), we examined the requirement for YAP in MYC overexpression-induced BEZ235 resistance in 2D. shRNA knockdown of endogenous YAP significantly sensitized MYC-overexpressing parental MCAS cells to BEZ235-induced proliferative suppression (Fig. 2E and Supplemental Fig. 2E, $p < 0.01$), indicating that the ability of MYC to drive proliferation under conditions of PI3K/mTOR inhibition is supported by endogenous YAP.

Endogenous YAP levels were unaffected by MYC expression, and vice versa (Supplemental Fig. 2F), indicating that co-dependence of these proteins is not due to direct regulation of one protein by the other. Therefore we focused on identifying other potential upstream mechanisms by which these proteins could be coordinately upregulated during the establishment of resistance. The p38/MAPK, which is known to regulate stress responses

when activated by phosphorylation (reviewed in (27)), was also identified by RPPA analysis as differentially regulated by BEZ235 in MCAS-R and MCAS-S cells (Fig. 2A and B). Given the known role of p38 in regulating response to cellular stress and cell cycle arrest (28), and its role in regulating YAP levels (29, 30), we examined whether it could contribute to enhanced proliferation of MCAS-R cells in 3D. Of note, although BEZ235 treatment induced activation of p38 (phosphorylation of T180/T182) in both MCAS-R and MCAS-S cells in 3D (Fig. 2A and B, Fig. 3A), MCAS-R cells displayed significantly less induction of phospho-p38 than MCAS-S cells (Figs. 2A and B, 3A), raising the possibility that reduced activation of p38 could contribute to the increased proliferative capacity of MCAS-R cells in the presence of BEZ235.

To examine the contribution of p38 to BEZ235 sensitivity, we inhibited p38 with SB203580 in parental MCAS cells treated with BEZ235 in 2D. This treatment significantly enhanced proliferation ($p < 0.05$) of BEZ235-treated cells, but had no effect on proliferation in the absence of BEZ235 (Fig. 3B and C, and Supplemental Fig. 3A). After 14d treatment, few cells remained in the BEZ235-treated samples, whereas small colonies of proliferating cells were apparent in samples treated with combined BEZ235 and p38 inhibitor (Fig. 3B). Combination treatment induced upregulation of YAP and MYC in parental MCAS cells (Fig. 3D and Supplemental Fig. 3B), as did BEZ235 treatment in combination with a structurally distinct p38 inhibitor (SB202190) (Supplemental Fig. 3C), indicating that in the presence of BEZ235, inhibition of p38 is sufficient to induce upregulation of YAP and MYC and result in proliferation.

Given that PI3K inhibition induces DNA damage (31, 32), a known regulator of p38 (27), we examined potential markers of DNA damage in the RPPA. We found that expression of XRCC1, Mre11 and X53BP1 was induced in the BEZ235-treated MCAS-S cells, whereas these proteins were all down-regulated in MCAS-R cells (Supplemental Fig. 3D). We next assessed the extent of DNA damage by phospho- γ H2AX immunofluorescence. BEZ235-treated MCAS-S cells displayed significantly more phospho- γ H2AX-positive foci compared to MCAS-R cells (Supplemental Fig. 3E), raising the possibility that DNA damage induced by PI3K/mTOR inhibition drives activation of p38 in MCAS-S cells, and that, through an unknown mechanism, this stress is resolved in MCAS-R cells.

To determine which node of the PI3K/mTOR-pathway regulates p38-activation, we treated parental MCAS cells in 2D with Torin1 (mTORi), BEZ235 (PI3Ki/mTORi), MK2206 (AKTi), GDC0941 (PI3Ki), or BKM120 (PI3Ki). Activation of p38 was not detected after short-term treatment (5min), indicating that a long-term inhibition is required for p38 activation. After 72h incubation, mTOR inhibition (BEZ235 or Torin1) induced robust phospho-p38, whereas AKT and PI3K inhibition induced it to a lesser extent (Supplemental Fig. 3F). A detailed time-course demonstrated that phospho-p38 was detectable after 3h incubation and reached a peak after 72h (Supplemental Fig. 3F). These data suggest that p38 activation in response to mTOR inhibition is not mediated by an acute kinase/phosphatase-cascade, but rather a mechanism that involves prolonged mTOR inhibition.

Interestingly, inhibition of p38 stabilizes cAMP response element-binding protein (CREB), which has been shown to positively regulate YAP levels (29, 30). To address whether CREB

could contribute to YAP upregulation in MCAS-R cells in 3D, we analyzed total CREB levels in the MCAS lines after BEZ235 treatment. We detected a marked increase in CREB protein levels in BEZ235-treated MCAS-R cells, whereas only a slight increase in MCAS-S cells was observed (Fig. 3E). Prolonged BEZ235 treatment (14d) of the parental MCAS cell line in 2D led to a marked increase in phospho-p38 and a decrease in CREB levels, and conversely p38 inhibition restored CREB levels in the parental BEZ235-treated cells (Fig. 3D and Supplemental Fig. 3C). These results are consistent with a model in which p38 activity, which is induced by BEZ235, suppresses CREB protein expression in the sensitive/parental cells.

To assess whether an increase in CREB protein levels is sufficient to promote resistance to mTOR inhibitors, we overexpressed wild-type CREB in parental MCAS cells and assessed proliferation in 2D. Overexpression of CREB significantly ($p<0.005$) increased the proliferation of BEZ235-treated parental MCAS cells and induced upregulation of YAP and MYC but only under BEZ235 treatment (Fig. 3F and G and Supplemental Fig. 3G). These results suggest that reduced p38 activation contributes both to the increase in proliferation and the upregulation of MYC, YAP and CREB levels observed in BEZ235-treated MCAS-R cells.

To evaluate the requirement for YAP downstream of CREB, we knocked down YAP in CREB-overexpressing parental MCAS cells. YAP depletion prevented proliferation in the presence of BEZ235, suggesting that YAP is required for CREB-induced proliferation under conditions of PI3K/mTOR inhibition (Fig. 3H). Furthermore, a comparative analysis of *CREB*-amplified versus non-amplified high-grade serous ovarian tumors revealed that YAP protein expression is significantly increased in tumors harboring *CREB* amplification ($p=0.031$, Fig. 3I). We also noted a significant positive correlation between *CREB* and *YAP* mRNA expression in colon, kidney, breast and liver tumors, suggesting that these proteins could be functionally coupled in patient tumors (Fig. 3J).

To assess whether YAP and MYC are required for resistance to PI3K/mTOR inhibitors in other cell lines, we analyzed a wide panel of tumor cell lines and identified three resistant lines that display continuous proliferation in the presence of BEZ235: the colon cancer cell line HCT116, and the ovarian cancer lines OVCAR5 and OvCa432 (Fig. 4A and Supplemental Fig. 4A and B). Notably, upregulation of YAP after six-day BEZ235 treatment was specifically observed in all resistant cell lines, and upregulation of MYC in HCT116 and OVCAR5 cells, but not in the sensitive lines (HeLa, MCF7 and TOV21G) (Fig. 4B). Although CREB upregulation was not detected following BEZ235 treatment, high basal CREB levels were specifically observed in the resistant cell lines (Fig. 4C). Furthermore, shRNA knockdown of either MYC or YAP significantly retarded proliferation in BEZ235-treated HCT116 cells ($p<0.001$), the most resistant cell line we identified (Fig. 4D and Supplemental Fig. 4C). We also found that transient overexpression of constitutively active p38 α significantly reduced the viability of HCT116 cells two days after BEZ235 treatment ($p<0.005$, Fig. 4E), suggesting that activation of p38 also sensitizes intrinsically resistant cells to PI3K/mTOR inhibition.

To assess whether PI3K/mTOR inhibition induces YAP and MYC upregulation *in vivo*, NOD-SCID mice were subcutaneously injected with resistant HCT116 and OVCAR5 cells and, once tumors were formed, were treated with vehicle or PI3K/mTOR inhibitor GNE493 (10mg/kg) (33). GNE493 treatment significantly increased intensity of both YAP (Fig. 5A and C) and MYC staining (Fig. 5B and D) in the Ki67-positive areas of HCT116 and OVCAR5 tumors (Fig. 5E), indicating that both YAP and MYC are upregulated in proliferating tumor cells *in vivo* under PI3K/mTOR inhibition.

To determine whether resistance to mTOR inhibitors is correlated with mutational status, we performed a proliferation analysis on a panel of cancer cell lines in the presence of mTOR inhibition (Fig. 6A). The proliferation index and resistance to mTOR inhibitors correlated with the mutational status of the KRAS/ERK-pathway (Fig. 6B). Of the resistant cell lines we previously identified, MCAS, HCT116, OVCAR5 and OVCA432 harbor activating mutations in KRAS (G12V). Consistent with these results, knockdown of KRAS sensitized HCT116 cells to PI3K/mTOR inhibition (Fig. 6C). Moreover, combined treatment of HCT116 cells with BEZ235 and 10μM MEK inhibitor (UO126) prevented upregulation of MYC and YAP, suggesting that RAS/MEK/ERK-pathway is required for MYC and YAP upregulation (Fig. 6D).

A role for ERK in mediating resistance to PI3K inhibitors has been reported (6, 11, 12). Given our data showing a correlation between PI3K/mTOR inhibitor resistance and KRAS mutational status, and that MYC and YAP upregulation was blocked by inhibition of the MEK/ERK-pathway, we probed for ERK activation in HCT116, MCAS-S and MCAS-R cells. BEZ235 treatment induced significant increase in phospho-ERK levels, including MCAS-S cells (Fig. 6E), suggesting that ERK activation alone is not sufficient to induce MYC and YAP upregulation. Since ERK can regulate CREB (34), we examined whether ERK inhibition positively or negatively affects CREB expression in resistant HCT116 and MCAS-R cells. Combined treatment with BEZ235 and UO126 inhibited CREB expression (Fig. 6F), suggesting that ERK activation is required for CREB expression in the resistant cells, and that p38 and ERK have opposing roles in the regulation of CREB protein levels.

Given the opposing effects of p38 and ERK on BEZ235 responsiveness, we next assessed the degree to which these pathways contribute to the acquired and intrinsic resistance. To do this, we evaluated the effects of p38 inhibition in combination with BEZ235 and UO126 on survival and MYC and YAP upregulation in HCT116 and parental MCAS cells. Unlike in the MCAS cells, the addition of p38 inhibitor with BEZ235 did not result in any additional upregulation of MYC and YAP in HCT116 cells. However, the addition of p38 inhibitor to BEZ235 and UO126 treatment resulted in significantly improved cell survival and upregulation of MYC and YAP in both cell lines (Fig. 6G and H). These data imply that, even in a KRAS mutant background, the efficacy of combined inhibition of the PI3K/mTOR- and MEK/ERK-pathways can be enhanced by the activation of p38, and conversely, that suppression of p38 can promote resistance through upregulation of MYC and YAP. Interestingly, combined treatment with p38 inhibitor and UO126 also resulted in improved cell survival (Figure 6G and H, Supplemental Fig. 4D), suggesting that activation of p38 could also be an effective strategy to improve responsiveness to MEK/ERK inhibitors in KRAS mutant tumors.

Taken together, these data support a model (Fig. 7) in which ERK and p38 play opposing roles in regulating the transcription factor CREB in tumor cells carrying mutations in the RAS/ERK-pathway, with ERK promoting CREB protein expression and p38 destabilizing it. Elevated CREB expression positively regulates YAP and MYC, allowing tumor cells to escape from proliferative suppression imposed by PI3K/mTOR inhibitors.

Discussion

Our data provide evidence for a previously unrecognized mode of drug resistance to PI3K/mTOR inhibitors, which is observed in both acquired and intrinsically resistant cell lines, that involves re-wiring several parallel signaling pathways that coordinately promote induction of YAP and MYC, both of which are required for proliferation under conditions of PI3K/mTOR inhibition (Fig. 7). Furthermore, our data support a model (Fig. 7) in which both the ERK and p38/MAPK-pathways play critical, dichotomous roles in regulating resistance.

In cells that are sensitive to PI3K/mTOR inhibitors, drug treatment induces cytostasis (Fig. 7A). This is likely mediated in part through p38 activation, which regulates cell cycle arrest at G1/S and G2/M checkpoints (28, 35). Our data indicate that suppression of p38 activity (Fig. 7C) allows resistant cells to escape proliferation inhibition induced by PI3K/mTOR inhibitors. This conclusion is supported by several findings: 1) p38-activation positively correlated with proliferation suppression by PI3K/mTOR inhibitors, 2) p38 activity was significantly lower in resistant cells compared to sensitive cells, and 3) p38 kinase inhibitors promoted proliferation, and YAP and MYC expression in the presence of BEZ235. Furthermore, p38 has been shown to regulate MYC expression at the post-transcriptional level (36), potentially explaining why MYC levels increased after combined BEZ235 and p38 inhibitor treatment. These data suggest that reduction in p38 activation in tumor cells could both release negative controls on proliferation as well as induce positive regulators of proliferation.

Our findings indicate that the mechanism of YAP upregulation upon p38 inhibition involves the transcription factor CREB. A recent report described an auto-regulatory feedback loop between p38, CREB and YAP whereby p38 inhibition leads to CREB stabilization (37). It was also shown that CREB binds to the YAP promoter and enhances its transcription (29, 30). Indeed, we observed that overexpression of CREB increased YAP levels, and inhibition of p38 led to increased CREB and YAP expression, suggesting a functional link between p38, CREB and YAP. Furthermore, TCGA database analysis showed positive correlation between CREB and YAP expression in several tumor datasets, suggesting that these proteins could also be functionally coupled in patient tumors.

p38 is activated in response to cellular stress, such as DNA damage (reviewed in (27)), and also in response to inhibition of oncogenic kinases, such as EGFR, Bcr-Abl and Src (38). Although our data do not delineate how p38 activity is suppressed in the resistant cells, our results and that of others suggest that acute PI3K/mTOR inhibition leads to DNA damage and activation of DNA repair pathways (31, 32). However, in the resistant cells, p38 activity

was significantly suppressed, as were markers of DNA repair, suggesting that these cells have resolved the DNA damage stress leading to p38 activation.

Our study also implicates the RAS/ERK-pathway in promoting drug resistance and upregulation of YAP and MYC by three findings: 1) the strong correlation between mutations in KRAS/BRAF and resistance to PI3K/mTOR inhibition, 2) the suppression of YAP, MYC and CREB expression in resistant cells treated with a MEK inhibitor, and 3) the loss of resistance induced by down-regulation of mutant KRAS in HCT116 cells. These results suggest that the activity of MEK/ERK-pathway positively influences resistance, and that mutations in the RAS pathway provide a context in which a MYC-YAP resistance mechanism can be operative. Furthermore, ERK-pathway has been shown to stabilize MYC protein (39, 40), and the RAS-pathway has been implicated in YAP protein stabilization (41). However, YAP has been shown to promote resistance to RAF/MEK-targeted cancer therapies in RAS mutant tumors (42, 43) and to rescue cancer cells after KRAS loss (44, 45), suggesting that YAP can be regulated at several levels to promote resistance to multiple targeted therapies.

Interestingly, both p38 and ERK-pathway activity, as well as reduced PI3K/AKT-pathway activity, have been linked to tumor cell dormancy (46–49). Results from the Aguirre-Ghisso group and others have shown that dormancy of tumor cells is dependent on the ratio of ERK and p38 activity, where a higher ERK/p38 ratio leads to cell cycle re-entry, whereas a higher p38/ERK ratio leads to tumor dormancy (50–53). Using a tumor model driven by *HER2*, Chodosh and colleagues showed that although withdrawal of this oncogene results in tumor regression, mice ultimately develop recurrent tumors that have become *HER2* independent (54), suggesting the existence of residual dormant tumor cells. Although Notch signaling was implicated in maintenance of dormancy, its inhibition did not inhibit tumor re-growth (55), suggesting that another pathway regulates the growth of recurrent tumors.

Chronic PI3K/mTOR inhibition might induce a state resembling dormancy, perhaps through activation of p38 and cell cycle arrest (Fig. 7A). However, in the context of a mutated RAS/ERK-pathway, and another unidentified factor that results in down-regulation of phospho-p38, the balance between p38 and ERK is shifted, and ERK becomes more dominant under PI3K/mTOR inhibition. The reduction in p38 leads to an increase in CREB, YAP, and MYC levels, allowing a low level of proliferation resembling ‘awakening’ from dormancy (Fig. 7B and C). We speculate that while the acquired resistance is mainly driven by suppressed p38 signaling, the intrinsic resistance would be more dependent on active ERK signaling. However, p38 inhibition in combination with PI3K/mTOR and MEK inhibitors resulted in improved fitness in both models, suggesting that activation of p38 would also benefit KRAS mutant tumors, a possibility worth exploring because of its translational implications.

In conclusion, these data suggest that in the absence of PI3K/mTOR signaling, MYC and YAP can orchestrate the required steps for cellular growth and proliferation normally driven by the PI3K/mTOR-pathways. We also demonstrate that activation of the RAS/ERK-pathway alone is not sufficient to allow proliferation in the presence of chronic PI3K/mTOR inhibition, but also requires suppression of the stress-activated p38/MAPK. This implies that

tumors treated with PI3K/mTOR inhibitors enter a state similar to tumor dormancy, and can evade therapies aimed at targeting proliferating cells.

Supplementary Material

Refer to Web version on PubMed Central for supplementary material.

Acknowledgments

Financial support: Source and number of grants for each author T. Muranen: NIC-5K99CA180221 and Laura Ziskin Memorial Award (Entertainment Industry Foundation); J.S. Brugge: gift from the Dr. Miriam and Sheldon G. Adelson Medical Research Foundation; D.M. Sabatini: NIH (R01 CA103866 and AI47389); G.B. Mills: 0099031 U54CA112970, BCRF 01-06-00332, Komen Foundation (KG08169404 and SAC110052), MDACC CCSG grant P30 CA016672, and a gift from the Dr. Miriam and Sheldon G. Adelson Medical Research Foundation.

We thank Dennis Slamon for providing cell lines; Jennifer Waters and Nikon Imaging Center at Harvard Medical School for assistance with microscopy; Deepak Sampath (Genentech) for providing GNE493; Julio Aguirre-Ghiso for providing p38 α construct; Angie Martinez-Gakidis for critical reading of the manuscript; Valerie Pireaux for technical help; Shomit Sengupta, and members of the Brugge lab for helpful discussions.

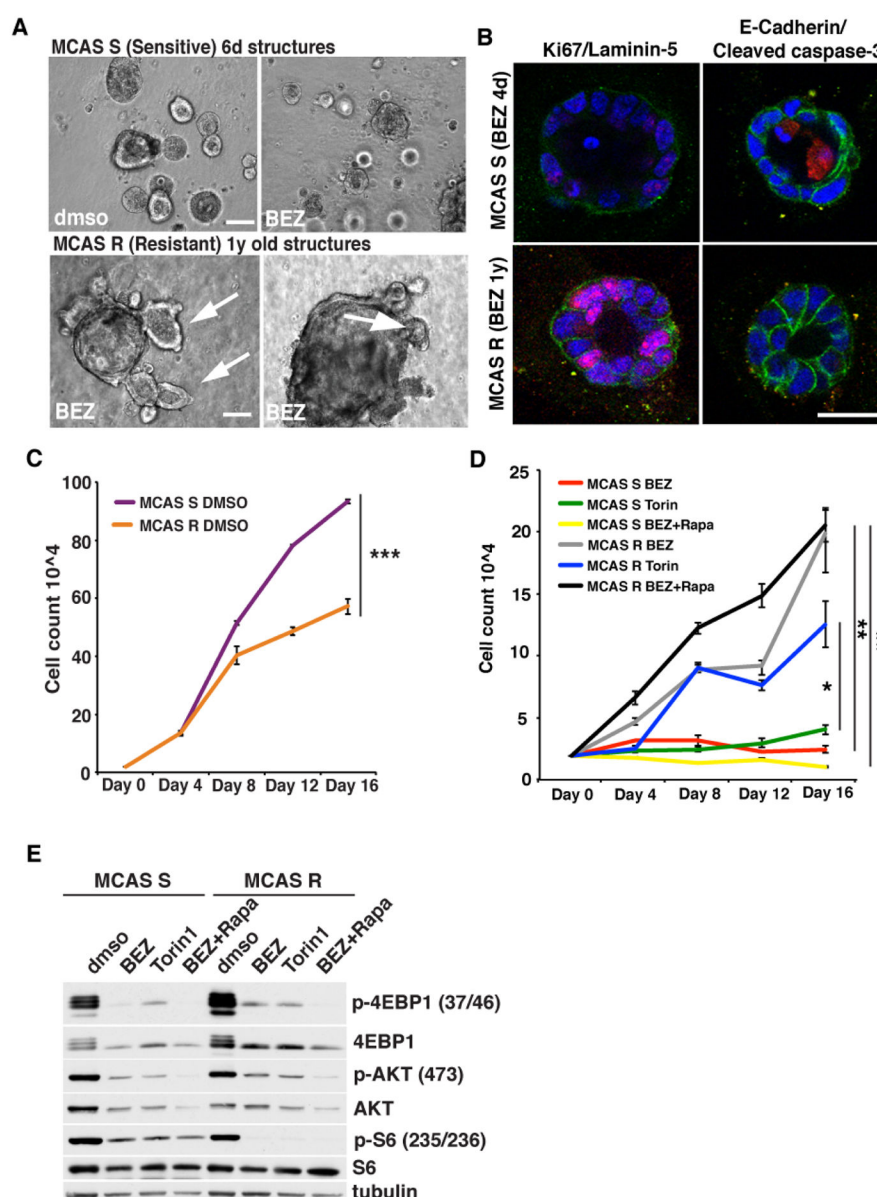
References

1. Dibble CC, Manning BD. Signal integration by mTORC1 coordinates nutrient input with biosynthetic output. *Nat Cell Biol.* 2013; 15:555–64. [PubMed: 23728461]
2. Engelman JA. Targeting PI3K signalling in cancer: opportunities, challenges and limitations. *Nat Rev Cancer.* 2009; 9:550–62. [PubMed: 19629070]
3. Samuels Y, Velculescu VE. Oncogenic mutations of PIK3CA in human cancers. *Cell Cycle.* 2004; 3:1221–4. [PubMed: 15467468]
4. Rodon J, Dienstmann R, Serra V, Tabernero J. Development of PI3K inhibitors: lessons learned from early clinical trials. *Nat Rev Clin Oncol.* 2013; 10:143–53. [PubMed: 23400000]
5. Chandarlapaty S, Sawai A, Scaltriti M, Rodrik-Outmezguine V, Grbovic-Huezo O, Serra V, et al. AKT Inhibition Relieves Feedback Suppression of Receptor Tyrosine Kinase Expression and Activity. *Cancer Cell.* 2011; 19:58–71. [PubMed: 21215704]
6. Serra V, Scaltriti M, Prudkin L, Eichhorn PJA, Ibrahim YH, Chandarlapaty S, et al. PI3K inhibition results in enhanced HER signaling and acquired ERK dependency in HER2-overexpressing breast cancer. *Oncogene.* 2011; 30:2547–57. [PubMed: 21278786]
7. Garrett JT, Olivares MG, Rinehart C, Granja-Ingram ND, Sánchez V, Chakrabarty A, et al. Transcriptional and posttranslational up-regulation of HER3 (ErbB3) compensates for inhibition of the HER2 tyrosine kinase. *Proc Natl Acad Sci USA.* 2011; 108:5021–6. [PubMed: 21385943]
8. Muranen T, Selfors LM, Worster DT, Iwanicki MP, Song L, Morales FC, et al. Inhibition of PI3K/mTOR leads to adaptive resistance in matrix-attached cancer cells. *Cancer Cell.* 2012; 21:227–39. [PubMed: 22340595]
9. Sergina NV, Rausch M, Wang D, Blair J, Hann B, Shokat KM, et al. Escape from HER-family tyrosine kinase inhibitor therapy by the kinase-inactive HER3. *Nature.* 2007; 445:437–41. [PubMed: 17206155]
10. O'Reilly KE, Rojo F, She Q-B, Solit D, Mills GB, Smith D, et al. mTOR inhibition induces upstream receptor tyrosine kinase signaling and activates Akt. *Cancer Res.* 2006; 66:1500–8. [PubMed: 16452206]
11. Carracedo A, Ma L, Teruya-Feldstein J, Rojo F, Salmena L, Alimonti A, et al. Inhibition of mTORC1 leads to MAPK pathway activation through a PI3K-dependent feedback loop in human cancer. *J Clin Invest.* 2008; 118:3065–74. [PubMed: 18725988]
12. Engelman JA, Chen L, Tan X, Crosby K, Guimaraes AR, Upadhyay R, et al. Effective use of PI3K and MEK inhibitors to treat mutant Kras G12D and PIK3CA H1047R murine lung cancers. *Nat Med.* 2008; 14:1351–6. [PubMed: 19029981]

13. Serra V, Eichhorn PJ, Garcia-Garcia C, Ibrahim YH, Prudkin L, Sanchez G, et al. RSK3/4 mediate resistance to PI3K pathway inhibitors in breast cancer. *J Clin Invest.* 2013; 123:2551–63. [PubMed: 23635776]
14. Liu P, Cheng H, Santiago S, Raeder M, Zhang F, Isabella A, et al. Oncogenic PIK3CA-driven mammary tumors frequently recur via PI3K pathway-dependent and PI3K pathway-independent mechanisms. *Nat Med.* 2011; 17:1116–20. [PubMed: 21822287]
15. Ilic N, Utermark T, Widlund HR, Roberts TM. PI3K-targeted therapy can be evaded by gene amplification along the MYC-eukaryotic translation initiation factor 4E (eIF4E) axis. *Proc Natl Acad Sci USA.* 2011; 108:E699–708. [PubMed: 21876152]
16. Tenbaum SP, Ordóñez-Morán P, Puig I, Chicote I, Arqués O, Landolfi S, et al. β -catenin confers resistance to PI3K and AKT inhibitors and subverts FOXO3a to promote metastasis in colon cancer. *Nat Med.* 2012; 18:892–901. [PubMed: 22610277]
17. Cope CL, Gilley R, Balmanno K, Sale MJ, Howarth KD, Hampson M, et al. Adaptation to mTOR kinase inhibitors by amplification of eIF4E to maintain cap-dependent translation. *J Cell Sci.* 2014; 127:788–800. [PubMed: 24363449]
18. Alain T, Morita M, Fonseca BD, Yanagiya A, Siddiqui N, Bhat M, et al. eIF4E/4E-BP ratio predicts the efficacy of mTOR targeted therapies. *Cancer Research.* 2012; 72:6468–76. [PubMed: 23100465]
19. Ducker GS, Atreya CE, Simko JP, Hom YK, Matli MR, Benes CH, et al. Incomplete inhibition of phosphorylation of 4E-BP1 as a mechanism of primary resistance to ATP-competitive mTOR inhibitors. *Oncogene.* 2014; 33:1590–600. [PubMed: 23542178]
20. Dowling RJO, Topisirovic I, Alain T, Bidinosti M, Fonseca BD, Petroulakis E, et al. mTORC1-mediated cell proliferation, but not cell growth, controlled by the 4E-BPs. *Science.* 2010; 328:1172–6. [PubMed: 20508131]
21. Hennessy BT, Lu Y, Gonzalez-Angulo AM, Carey MS, Myhre S, Ju Z, et al. A Technical Assessment of the Utility of Reverse Phase Protein Arrays for the Study of the Functional Proteome in Non-microdissected Human Breast Cancers. *Clin Proteomics.* 2010; 6:129–51. [PubMed: 21691416]
22. Ory DS, Neugeboren BA, Mulligan RC. A stable human-derived packaging cell line for production of high titer retrovirus/vesicular stomatitis virus G pseudotypes. *Proc Natl Acad Sci U S A.* 1996; 93:11400–6. [PubMed: 8876147]
23. Debnath J, Muthuswamy SK, Brugge JS. Morphogenesis and oncogenesis of MCF-10A mammary epithelial acini grown in three-dimensional basement membrane cultures. *Methods.* 2003; 30:256–68. [PubMed: 12798140]
24. Carson AR, Smith EN, Matsui H, Braekkan SK, Jepsen K, Hansen JB, et al. Effective filtering strategies to improve data quality from population-based whole exome sequencing studies. *BMC Bioinformatics.* 2014; 15:125. [PubMed: 24884706]
25. Tumaneng K, Russell Ryan C, Guan K-L. Organ Size Control by Hippo and TOR Pathways. *Curr Biol.* 2012; 22:R368–R79. [PubMed: 22575479]
26. Yu F-X, Guan K-L. The Hippo pathway: regulators and regulations. *Genes & Development.* 2013; 27:355–71. [PubMed: 23431053]
27. Coulthard LR, White DE, Jones DL, McDermott MF, Burchill SA. p38(MAPK): stress responses from molecular mechanisms to therapeutics. *Trends Mol Med.* 2009; 15:369–79. [PubMed: 19665431]
28. Reinhardt HC, Hasskamp P, Schmedding I, Morandell S, van Vugt MA, Wang X, et al. DNA damage activates a spatially distinct late cytoplasmic cell-cycle checkpoint network controlled by MK2-mediated RNA stabilization. *Mol Cell.* 2010; 40:34–49. [PubMed: 20932473]
29. Wang J, Ma L, Weng W, Qiao Y, Zhang Y, He J, et al. Mutual interaction between YAP and CREB promotes tumorigenesis in liver cancer. *Hepatology.* 2013; 58:1011–20. [PubMed: 23532963]
30. Zhang T, Zhang J, You X, Liu Q, Du Y, Gao Y, et al. Hepatitis B virus X protein modulates oncogene Yes-associated protein by CREB to promote growth of hepatoma cells. *Hepatology.* 2012; 56:2051–9. [PubMed: 22707013]

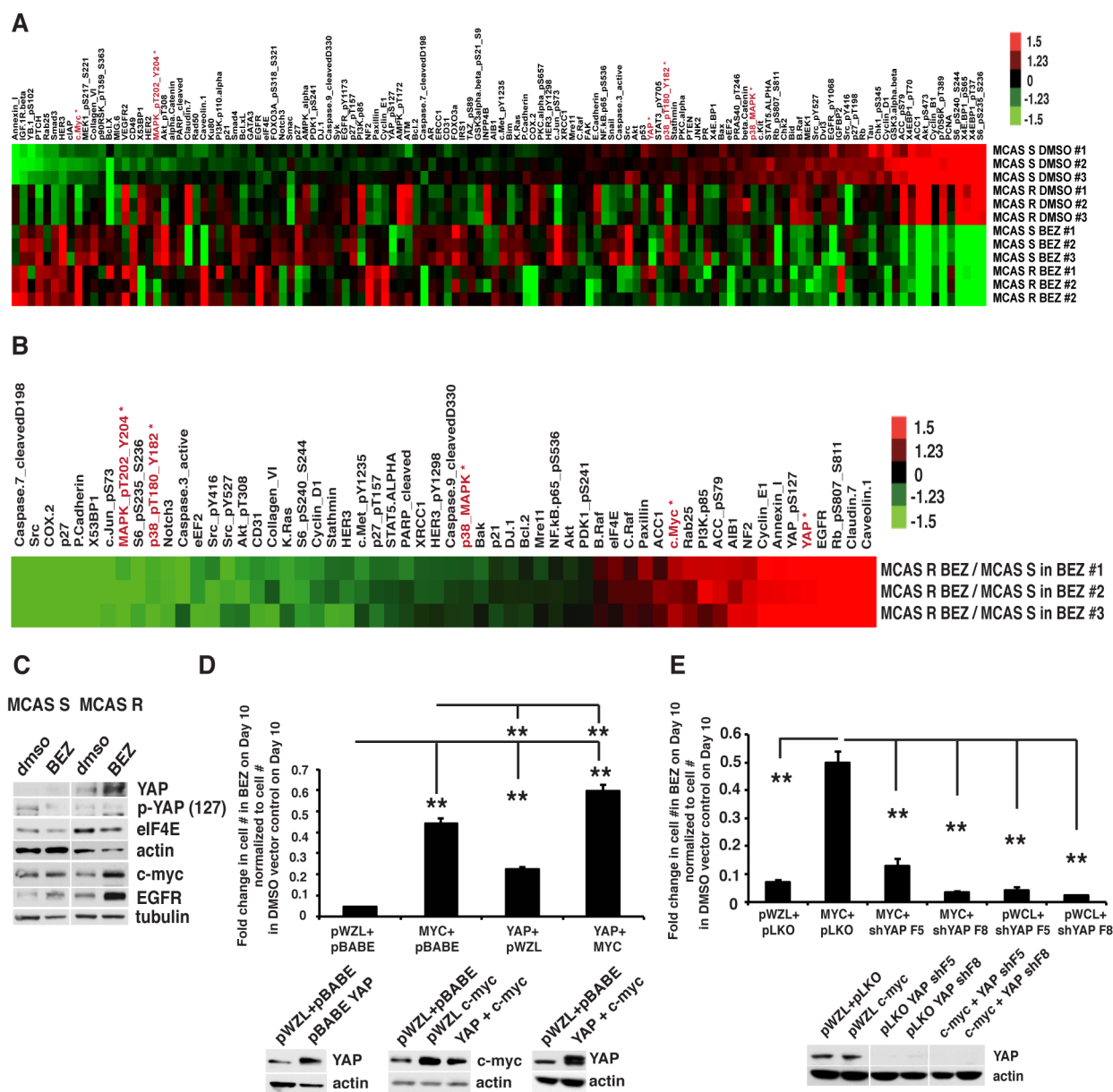
31. Juvekar A, Burga LN, Hu H, Lunsford EP, Ibrahim YH, Balmana J, et al. Combining a PI3K inhibitor with a PARP inhibitor provides an effective therapy for BRCA1-related breast cancer. *Cancer Discov.* 2012; 2:1048–63. [PubMed: 22915751]
32. Ibrahim YH, Garcia-Garcia C, Serra V, He L, Torres-Lockhart K, Prat A, et al. PI3K inhibition impairs BRCA1/2 expression and sensitizes BRCA-proficient triple-negative breast cancer to PARP inhibition. *Cancer Discov.* 2012; 2:1036–47. [PubMed: 22915752]
33. Sutherlin DP, Sampath D, Berry M, Castanedo G, Chang Z, Chuckowree I, et al. Discovery of (thienopyrimidin-2-yl)aminopyrimidines as potent, selective, and orally available pan-PI3-kinase and dual pan-PI3-kinase/mTOR inhibitors for the treatment of cancer. *J Med Chem.* 2010; 53:1086–97. [PubMed: 20050669]
34. Deak M, Clifton AD, Lucocq LM, Alessi DR. Mitogen- and stress-activated protein kinase-1 (MSK1) is directly activated by MAPK and SAPK2/p38, and may mediate activation of CREB. *EMBO J.* 1998; 17:4426–41. [PubMed: 9687510]
35. Manke IA, Nguyen A, Lim D, Stewart MQ, Elia AE, Yaffe MB. MAPKAP kinase-2 is a cell cycle checkpoint kinase that regulates the G2/M transition and S phase progression in response to UV irradiation. *Mol Cell.* 2005; 17:37–48. [PubMed: 15629715]
36. Cannell IG, Kong YW, Johnston SJ, Chen ML, Collins HM, Dobbyn HC, et al. p38 MAPK/MK2-mediated induction of miR-34c following DNA damage prevents Myc-dependent DNA replication. *Proc Natl Acad Sci U S A.* 2010; 107:5375–80. [PubMed: 20212154]
37. Wang J, Park J-S, Wei Y, Rajurkar M, Cotton Jennifer L, Fan Q, et al. TRIB2 Acts Downstream of Wnt/TCF in Liver Cancer Cells to Regulate YAP and C/EBP α Function. *Molecular Cell.* 2013; 51:211–25. [PubMed: 23769673]
38. Sharma SV, Gajowniczek P, Way IP, Lee DY, Jiang J, Yuza Y, et al. A common signaling cascade may underlie “addiction” to the Src, BCR-ABL, and EGF receptor oncogenes. *Cancer Cell.* 2006; 10:425–35. [PubMed: 17097564]
39. Sears R, Leone G, DeGregori J, Nevins JR. Ras enhances Myc protein stability. *Mol Cell.* 1999; 3:169–79. [PubMed: 10078200]
40. Sears R, Nuckolls F, Haura E, Taya Y, Tamai K, Nevins JR. Multiple Ras-dependent phosphorylation pathways regulate Myc protein stability. *Genes & Development.* 2000; 14:2501–14. [PubMed: 11018017]
41. Hong X, Nguyen HT, Chen Q, Zhang R, Hagman Z, Voorhoeve PM, et al. Opposing activities of the Ras and Hippo pathways converge on regulation of YAP protein turnover. *EMBO J.* 2014; 33:2447–57. [PubMed: 25180228]
42. Lin L, Sabnis AJ, Chan E, Olivas V, Cade L, Pazarentzos E, et al. The Hippo effector YAP promotes resistance to RAF- and MEK-targeted cancer therapies. *Nat Genet.* 2015; 47:250–6. [PubMed: 25665005]
43. Kim MH, Kim J, Hong H, Lee SH, Lee JK, Jung E, et al. Actin remodeling confers BRAF inhibitor resistance to melanoma cells through YAP/TAZ activation. *EMBO J.* 2016; 35:462–78. [PubMed: 26668268]
44. Shao DD, Xue W, Krall EB, Bhutkar A, Piccioni F, Wang X, et al. KRAS and YAP1 converge to regulate EMT and tumor survival. *Cell.* 2014; 158:171–84. [PubMed: 24954536]
45. Kapoor A, Yao W, Ying H, Hua S, Liewen A, Wang Q, et al. Yap1 activation enables bypass of oncogenic Kras addiction in pancreatic cancer. *Cell.* 2014; 158:185–97. [PubMed: 24954535]
46. Jo H, Jia Y, Subramanian KK, Hattori H, Luo HR. Cancer cell-derived clusterin modulates the phosphatidylinositol 3'-kinase-Akt pathway through attenuation of insulin-like growth factor 1 during serum deprivation. *Mol Cell Biol.* 2008; 28:4285–99. [PubMed: 18458059]
47. Humtsoe JO, Kramer RH. Differential epidermal growth factor receptor signaling regulates anchorage-independent growth by modulation of the PI3K/AKT pathway. *Oncogene.* 2010; 29:1214–26. [PubMed: 19935697]
48. Balz LM, Bartkowiak K, Andreas A, Pantel K, Niggemann B, Zanker KS, et al. The interplay of HER2/HER3/PI3K and EGFR/HER2/PLC-gamma1 signalling in breast cancer cell migration and dissemination. *J Pathol.* 2012; 227:234–44. [PubMed: 22262199]
49. Schewe DM, Aguirre-Ghiso JA. ATF6 α -Rheb-mTOR signaling promotes survival of dormant tumor cells in vivo. *Proc Natl Acad Sci U S A.* 2008; 105:10519–24. [PubMed: 18650380]

50. Diehl NL, Enslen H, Fortner KA, Merritt C, Stetson N, Charland C, et al. Activation of the p38 mitogen-activated protein kinase pathway arrests cell cycle progression and differentiation of immature thymocytes in vivo. *J Exp Med*. 2000; 191:321–34. [PubMed: 10637276]
51. Aguirre-Ghiso JA, Estrada Y, Liu D, Ossowski L. ERK(MAPK) activity as a determinant of tumor growth and dormancy; regulation by p38(SAPK). *Cancer Res*. 2003; 63:1684–95. [PubMed: 12670923]
52. Aguirre-Ghiso JA, Ossowski L, Rosenbaum SK. Green fluorescent protein tagging of extracellular signal-regulated kinase and p38 pathways reveals novel dynamics of pathway activation during primary and metastatic growth. *Cancer Res*. 2004; 64:7336–45. [PubMed: 15492254]
53. Bragado P, Estrada Y, Parikh F, Krause S, Capobianco C, Farina HG, et al. TGF-beta2 dictates disseminated tumour cell fate in target organs through TGF-beta-RIII and p38alpha/beta signalling. *Nat Cell Biol*. 2013; 15:1351–61. [PubMed: 24161934]
54. Moody SE, Sarkisian CJ, Hahn KT, Gunther EJ, Pickup S, Dugan KD, et al. Conditional activation of Neu in the mammary epithelium of transgenic mice results in reversible pulmonary metastasis. *Cancer Cell*. 2002; 2:451–61. [PubMed: 12498714]
55. Abravanel DL, Belka GK, Pan TC, Pant DK, Collins MA, Sterner CJ, et al. Notch promotes recurrence of dormant tumor cells following HER2/neu-targeted therapy. *J Clin Invest*. 2015; 125:2484–96. [PubMed: 25961456]
56. Eckert LB, Repasky GA, Ulku AS, McFall A, Zhou H, Sartor CI, et al. Involvement of Ras activation in human breast cancer cell signaling, invasion, and anoikis. *Cancer Res*. 2004; 64:4585–92. [PubMed: 15231670]

**Figure 1.**

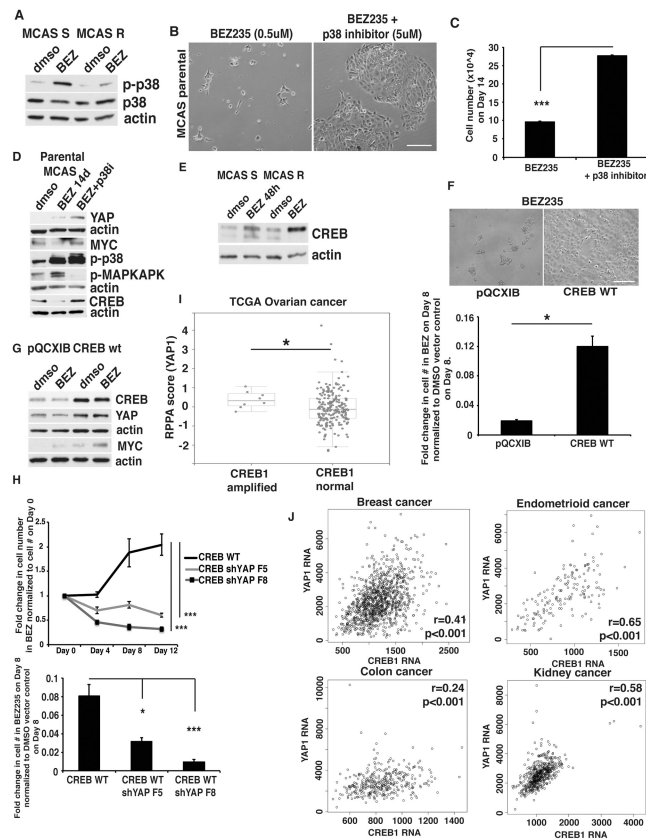
MCAS cancer cells develop resistance to chronic PI3K/mTOR inhibition. (A) Top panel: Representative images of sensitive (MCAS-S) spheroids incubated with BEZ235 for 2d. Bottom panel: Representative images of resistant (MCAS-R) spheroids incubated with 1 μ M BEZ235 for 1y. Outgrowths of proliferating cells were detected in multiple structures (arrows). Scale bar: 200 μ m. (B) Left panel: Ki67 (red) and Laminin-5 (green) staining of MCAS-S and MCAS-R cells in BEZ235. Right panel: Cleaved-caspase-3 (red) and E-cadherin (green) staining of resistant and sensitive cells. Scale bar: 25 μ m. (C–D) Cells were isolated from spheroid cultures, and similar numbers were re-plated in 3D. The MCAS-S and MCAS-R cells were incubated with DMSO (C), BEZ235 (0.5 μ M), Torin1 (0.5 μ M), or BEZ235 with Rapamycin (20nM) (D), proliferation was measured by cell counting. Data is

shown as total cell number and presented as mean SEM+/- from representative experiment of five. Statistical analysis: one-way ANOVA ($p < 0.001$) and post-hoc Tukey HSD test. Pairwise p-values are shown (** $p < 0.005$, ** $p < 0.01$, * $p < 0.05$). (E) Western blot analysis of mTOR downstream-effectors from MCAS-R and MCAS-S cells in 3D treated with DMSO, BEZ235, Torin, or BEZ+Rapamycin for 48h (MCAS-S) or 6d (MCAS-R).

**Figure 2.**

MCAS-R cells exhibit increased MYC and YAP expression. (A) Heatmap from reverse phase protein array (RPPA) analysis showing proteins/phospho-proteins differentially expressed in MCAS-S and MCAS-R lines following DMSO and BEZ235 treatment (ANOVA, $p < 0.05$). Data are median centered (red: greater than the median, green: less). For (A) and (B), the most discussed proteins in the manuscript are labeled in red font and marked with an asterisk. (B) RPPA analysis showing proteins differentially altered by BEZ235 in MCAS-S and MCAS-R cells in 3D. Heatmap visualizes relative differences in signal induced by BEZ235 in MCAS-R cells compared to BEZ235-treated MCAS-S cells. Proteins with significant (t-test, $p < 0.05$) changes are shown. Values from BEZ235-resistant line are normalized to the average of BEZ235-sensitive line. (C) Western-blot validation of

the 3D protein arrays from (A–B). (D) Parental MCAS cells in 2D were transduced with pBABE-YAP and/or pWZL-MYC or plasmid controls, incubated with BEZ235 and counted. Fold change in cell number was calculated by normalizing the number of cells counted on Day 10 in BEZ235 compared to number of cells on Day 10 in their own DMSO controls. Lower panel shows validation of MYC/YAP expression. Statistical analysis: one-way ANOVA ($p=6.1839e-14$) and Tukey's HSD test, which showed significant differences between all pairs $**p<0.01$. (E) YAP was knocked down with shRNAs (F5 and F8) in control or MYC-overexpressing MCAS cells and cell numbers were analyzed as in D. The proliferation graphs are a combined experiment of two, with triplicates in each. All data shown as mean SEM \pm . Statistical analysis: one-way ANOVA ($p=1.8652e-14$) with Tukey's HSD test. $**p<0.01$.

**Figure 3.**

p38 and CREB regulate MYC and YAP. (A) phospho-p38 (T180/Y182) and p38 were probed by Western blot from MCAS-R and MCAS-S cells in DMSO or BEZ235 in 3D for 6d. (B) Phase contrast images of parental MCAS cells cultured in 2D for 14 days in the presence of BEZ235 (BEZ), or pre-incubated with 5 μ M p38 inhibitor (SB203580) and then co-incubated with BEZ235. (C) Parental MCAS cells in 2D were treated with BEZ235 alone or BEZ235+SB203580 for 14d and cell numbers were counted on Day 14, graph represents total cell numbers. (D) Parental MCAS cells were incubated in 2D with DMSO, BEZ235 or combined BEZ235 and SB203580 for 14d, and lysates were probed for CREB, MYC, YAP, p-p38, and p-MAPKAPK by Western blot. (E) MCAS-S and MCAS-R cells were cultured in 3D with BEZ235 and DMSO as in (A), lysed and probed for CREB. (F) Parental MCAS cells expressing wild-type CREB or control were cultured in BEZ235 in 2D. Cells were imaged at Day 12, and counted at indicated time-points. Graph shows fold change in cell number in BEZ235 on Day 8 compared to its own vector control in DMSO on Day 8. (G) Western blot analysis of cells from (F). Lysates were probed for CREB, MYC, and YAP. (H) Parental MCAS cells overexpressing WT-CREB and YAP shRNAs were cultured in BEZ235 for the indicated time and [upper panel]: fold change in cell number over time in BEZ235 normalized over cell number on Day 0, or [lower panel]: determined and normalized as in F. (I) Comparative analysis of YAP protein levels (RPPA-score) in *CREB* amplified vs. non-amplified TCGA ovarian cancer data set. (J) Breast, endometrioid, colon and kidney cancer TCGA studies all show significant positive correlations between *CREB* and *YAP* mRNA

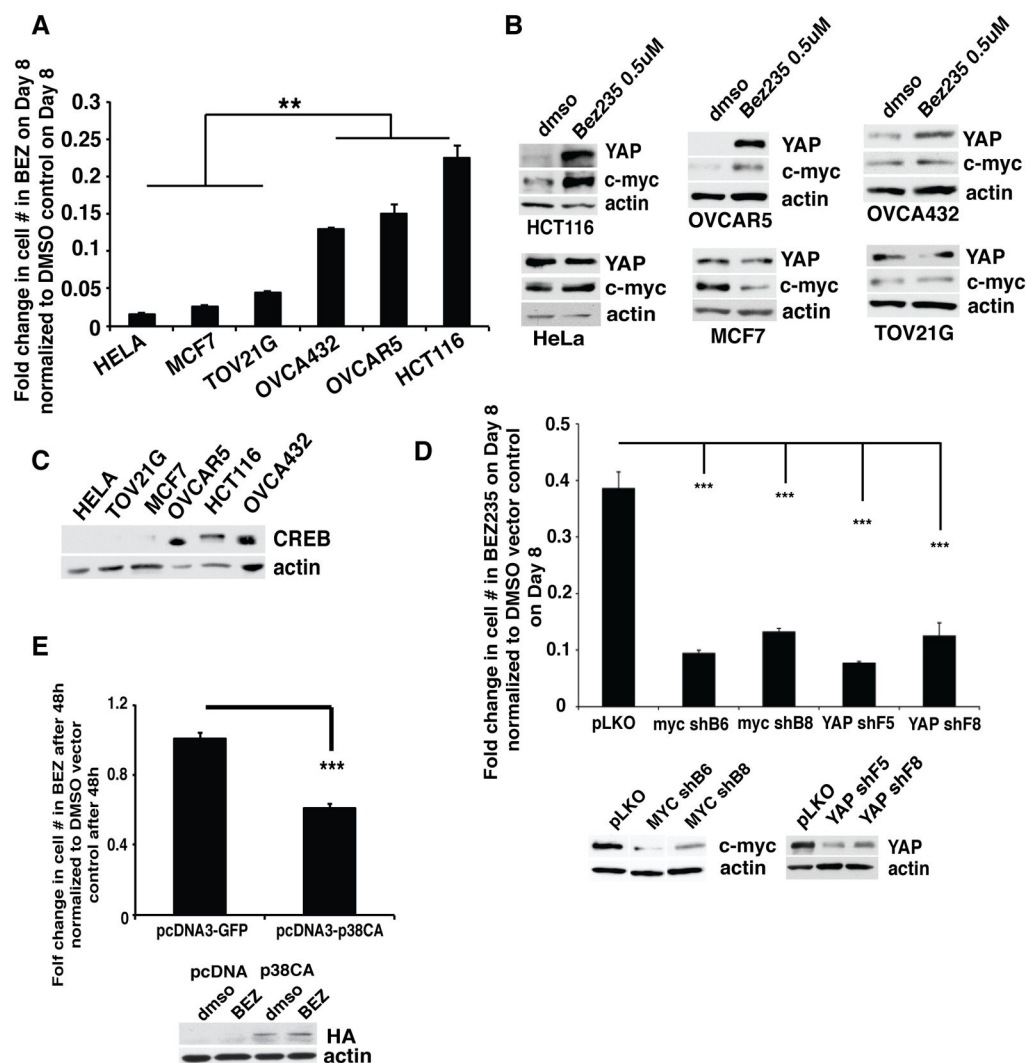
expression in human tumors. The proliferation graphs are a representative experiment of three, and triplicates were analyzed. All data shown as mean SEM \pm /. Statistical analysis: Student's t-test. * $p < 0.05$, ** $p < 0.01$, *** $p < 0.005$. Scale bars 100 μ m.

Author Manuscript

Author Manuscript

Author Manuscript

Author Manuscript

**Figure 4.**

Several intrinsically resistant tumor cell lines upregulate MYC and YAP in BEZ235. (A) Cell proliferation was measured for six cancer cell lines in the presence and absence of BEZ235 and represented as fold change in cell number in BEZ235 on Day 8 compared to the respective DMSO control on Day 8. (B) Western blot analysis of MYC and YAP in cell lines indicated in (A). (C) Cells were treated with BEZ235 for 8d and CREB levels were analyzed by Western blot. (D) MYC or YAP was knocked down by shRNAs (MYCsh: B6/B8; YAPsh: F5/F8) in HCT116 cells and change in cell number is shown as in (A) but each cell type is normalized to its own vector DMSO control. (E) HCT116 cells were transfected with pcDNA3-GFP or constitutively active p38 (pcDNA3-p38CA), treated with BEZ235 for 48h and cell proliferation was compared to proliferation in DMSO controls. All proliferation experiments were conducted with biological triplicates and repeated twice. All data shown as mean SEM+/- . Statistical analysis: Student's t-test. ***p<0.005, **p<0.01.

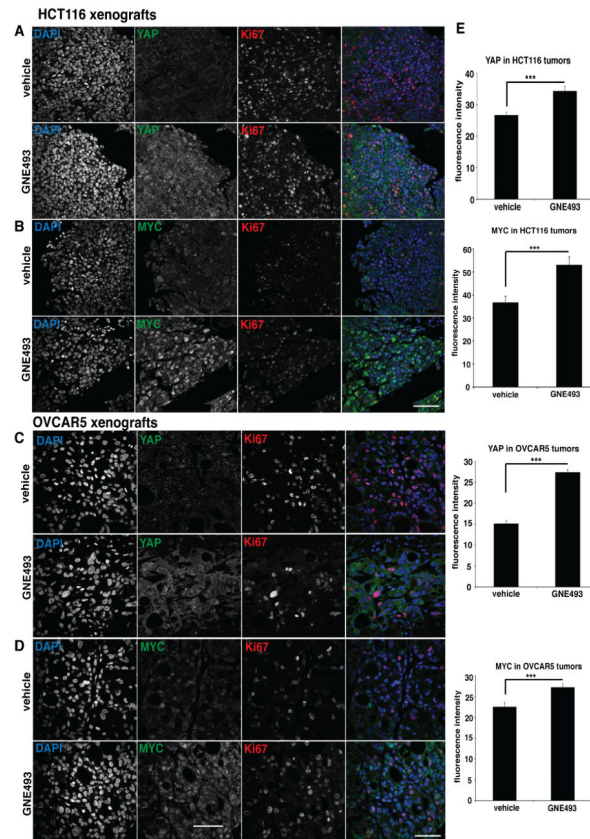
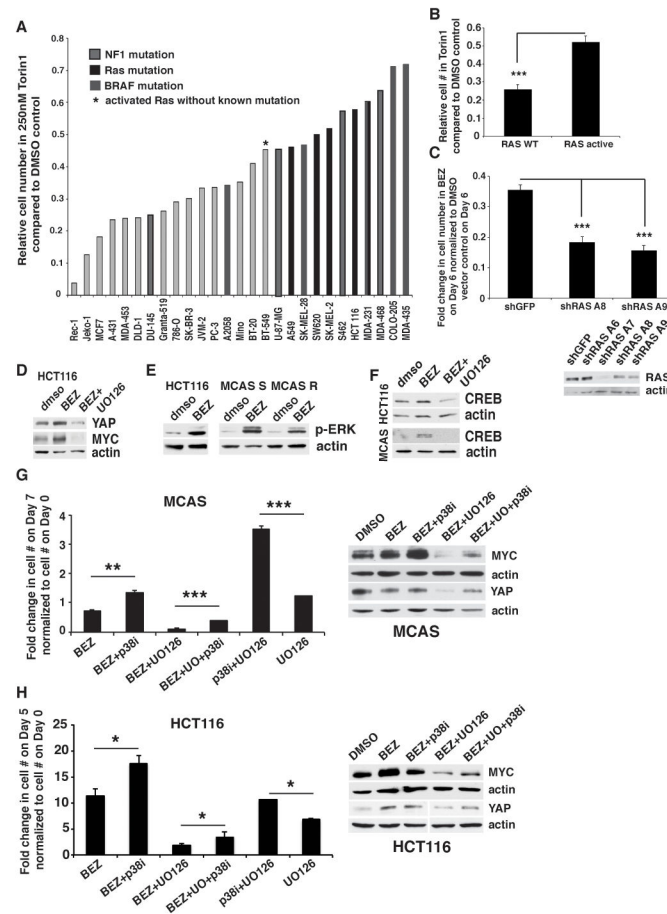


Figure 5.

YAP and MYC are upregulated in mTOR inhibitor-treated xenograft tumors. (A–B) HCT116 and (C–D) OVCAR5 cells were injected subcutaneously into five NOD-SCID mice and following tumor formation, mice were treated every 24h with PI3K/mTOR inhibitor GNE493 (10mg/kg) or vehicle for 8–14d. Tumors were harvested and stained for Ki67 (red) and MYC (B/D, green) or YAP (A/C, green). (E) Quantification of fluorescence intensity values of MYC and YAP staining in vehicle- and GNE493-treated tumors. Data shown as mean SEM \pm . Statistical analysis: Student's t-test. ***p<0.005, **p<0.01, *p<0.05. Scale bar 50μm.

**Figure 6.**

Activated KRAS-pathway promotes resistance. (A) Cell lines were cultured in 2D with mTOR inhibitor Torin1 for 6d and relative growth in Torin1 compared to DMSO is shown. Cell lines with *BRAF*, *RAS* or *NF1* mutation are indicated. *indicates cell line with activated RAS with no known mutation (56). (B) Relative cell number in Torin1 compared to DMSO in RAS-activated cells vs. non-RAS activated cells. (C) KRAS was knocked down in HCT116 cells and data is shown as fold change in cell number in BEZ235 on Day 6 compared to each vectors DMSO control on Day 6. Lower panel shows validation of RAS knockdown. KRAS shRNA A7 resulted in cell death in DMSO and could not be used. Proliferation experiment was done twice with triplicates. (D) HCT116 cells were cultured in 2D for 6 days in the presence of DMSO, BEZ235, or BEZ235 and 10 μ M UO126 and probed for MYC and YAP. (E) HCT116 in 2D and MCAS-R and -S cells in 3D were cultured for 48h with DMSO or BEZ235 and probed for p-ERK. (F) MCAS-R and HCT116 cells were grown with DMSO, 0.5 μ M BEZ235, or BEZ235 and UO126 (10 μ M). Lysates were collected after 48h and probed for CREB and actin. (G) Parental MCAS cells and (H) HCT116 cells were cultured in 2D with indicated inhibitors and counted on Day 0 and Day 5 (HCT116) or Day 7 (MCAS). Fold change in cell number was calculated by comparing the cell number at the end of the experiment to that on Day 0. Experiments were repeated twice with triplicates. Cells were lysed on Day 2 (MCAS) and Day 4 (HCT116) and probed for MYC, YAP, and

actin. All data shown as mean SEM+/- . Statistical analysis: Student's t-test. *p<0.05, **p<0.01, *** p<0.005.

Author Manuscript

Author Manuscript

Author Manuscript

Author Manuscript

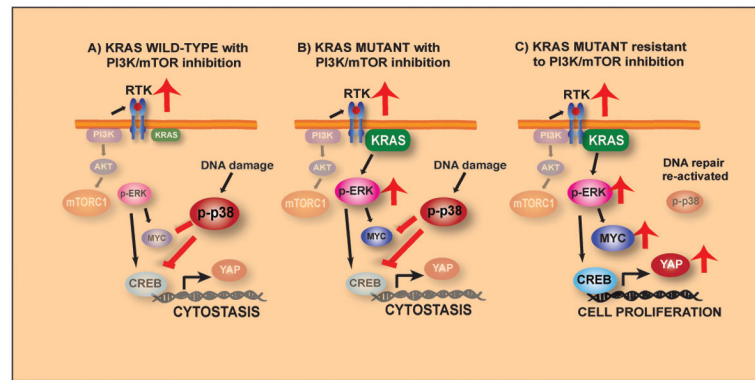


Figure 7.

Model of signaling events leading to MYC and YAP upregulation. (A) In KRAS WT cells, inhibition of PI3K/mTOR leads to up-regulation of p38 through activated DNA damage pathway (and inhibition of CREB and MYC), and upregulation of receptor tyrosine kinases, with only a minor increase in p-ERK. (B) In KRAS mutant background, increased MEK/ERK-signaling leads to slightly higher MYC levels, but high p-p38 still opposes MYC, CREB and YAP. (C) In KRAS mutant cells that have down-regulated p38 activity by relieving DNA damage response through an unknown mechanism, suppression of MYC and CREB is relieved and YAP is upregulated.